



## Research articles

Evolution of spatial spin-modulated structure with La doping in  $\text{Bi}_{1-y}\text{La}_y\text{FeO}_3$  multiferroicsV.S. Pokatilov<sup>a</sup>, A.O. Makarova<sup>a</sup>, A.A. Gippius<sup>b,c</sup>, A.V. Tkachev<sup>c</sup>, S.V. Zhurenko<sup>c</sup>, A.N. Bagdinova<sup>c</sup>, N.E. Gervits<sup>c,\*</sup><sup>a</sup> Moscow Technological University (MIREA), 119454 Moscow, Russia<sup>b</sup> Lomonosov Moscow State University, 119991 Moscow, Russia<sup>c</sup> Lebedev Physical Institute, Russian Academy of Sciences, 119991 Moscow, Russia

## ARTICLE INFO

## Keywords:

NMR spectroscopy  
Mössbauer spectroscopy  
Multiferroics  
Bismuth ferrite  
SSMS  
Magnetic anisotropy  
Anharmonicity

## ABSTRACT

In this paper we present study of the magnetic structure of multiferroic series  $\text{Bi}_{1-y}\text{La}_y\text{FeO}_3$  ( $y = 0, 0.015, 0.03, 0.05$  and  $0.10$ ) using nuclear magnetic resonance (NMR) at 4.2 K and Mössbauer spectroscopy at room temperature on  $^{57}\text{Fe}$  nuclei. We observed the presence of cycloid type spatial spin-modulated structure (SSMS) in the whole range of compositions. The study of the concentration dependence of the anharmonicity parameter  $m$  revealed that at the temperature of liquid helium in the composition region  $y = 0 - 0.10$  as well as at room temperature for  $y = 0.03$  the magnetic state of multiferroics is described by cycloid type SSMS with a positive effective uniaxial constant of magnetic anisotropy  $K_u > 0$  ("easy axis" model). The study at room temperature in turn revealed that magnetic state of the multiferroics with  $y = 0 - 0.03$  is described by cycloid type SSMS with a positive effective uniaxial constant of magnetic anisotropy  $K_u > 0$  ("easy axis" model). In contrast, the magnetic state of multiferroics with  $y = 0.05$  and  $0.10$  is described by a negative effective uniaxial constant of magnetic anisotropy  $K_u < 0$  ("easy plane" model). Anharmonicity parameter  $m$  at room temperature for  $y = 0.03 - 0.05$  is close to zero, which means that SSMS in this range of compositions is close to harmonic.

## 1. Introduction

Promising prospects of I type multiferroic  $\text{BiFeO}_3$  (BFO) application in spintronics, data storage and various multifunctional devices generate keen interest in BFO-based compounds over the past 30 years [1–4]. Pure undoped  $\text{BiFeO}_3$  possesses rhombohedral distorted perovskite structure (sp. gr.  $R3c$ ), high Curie temperature of 1100 K and Neel temperature of 670 K [5,6]. In paper [7] the authors observed a complicated cycloid type spatial spin-modulated structure (SSMS) with relatively big period  $\lambda = 620 \pm 20 \text{ \AA}$  incommensurate with the crystal lattice period by means of time-of-flight neutron diffractometry. Each magnetic moment of the trivalent iron ion  $\text{Fe}^{3+}$ , surrounded by neighbouring  $\text{Fe}^{3+}$  ions with spins antiparallel to the spin of the central atom, rotates along the direction of the modulated wave in a plane perpendicular to the hexagonal basal plane. The presence of SSMS reduces to zero the total magnetization and linear magnetoelectric effect [8]. One can conclude that for practical applications of these ferrites SSMS must be suppressed. Various methods for suppressing SSMS are described in the literature, for example, replacing bismuth or iron with other elements [8–10], synthesizing samples in the form of

nanocrystallites or thin films [2,11–13], and also using an external magnetic field [14,15].

The replacement of bismuth atoms by rare-earth atoms affects the physical properties (including magnetoelectric). This effect is due to the difference between ionic radii, valency and other parameters of  $\text{Bi}^{3+}$  ions and substitute ions [16]. It was shown in [17] that doping of BFO with lanthanum leads to a structural transition from the rhombohedral to the orthorhombic phase due to chemical compression. Evidence of a decrease in the concentration of charge defects, dielectric losses, and leakage current upon doping with La is given in [18,19]. It was also found that certain concentrations of various elements replacing bismuth lead to the destruction of SSMS in compounds based on BFO [11,20,21].

In [22], a mathematical description of SSMS in BFO is given through the function of the anharmonic cycloid:

$$\cos\theta(x) = \text{sn}\left(\pm \frac{4K(m)}{\lambda}x, m\right) \text{ at } K_u > 0 \quad (1)$$

$$\sin\theta(x) = \text{sn}\left(\pm \frac{4K(m)}{\lambda}x, m\right) \text{ at } K_u < 0 \quad (2)$$

\* Corresponding author.

E-mail address: [ngervits@gmail.com](mailto:ngervits@gmail.com) (N.E. Gervits).<https://doi.org/10.1016/j.jmmm.2020.167341>

Received 6 May 2020; Received in revised form 22 August 2020; Accepted 23 August 2020

Available online 05 September 2020

0304-8853/© 2020 Elsevier B.V. All rights reserved.

where  $\theta$  is the angle of rotation of the antiferromagnetism vector relative to the  $c$  axis;  $x$  is the coordinate along the direction of propagation of the cycloid;  $sn(x, m)$  is the Jacobi elliptic function with the anharmonicity parameter  $m$ ;  $K(m)$  is a complete elliptic integral of the first kind. The SSMS period  $\lambda$  is determined by the exchange stiffness  $A$ , the effective constant of the uniaxial magnetic anisotropy  $K_u$ , and the anharmonicity parameter  $m$  [22,23].

As follows from Eqs. (1), (2), the SSMS anharmonicity leads to a non-uniform distribution of the magnetic moments of iron over the angle  $\theta$ , leading to their higher concentration near the  $c$  axis or in the perpendicular direction, depending on the sign of the  $K_u$  magnetic anisotropy constant. Moreover, magnetic anisotropy also leads to a weak anisotropy of local hyperfine fields at the nuclei  $^{57}\text{Fe}$   $H_{\text{hf}}(\theta)$  [22,24]:

$$H_{\text{hf}}(\theta) = H_{\text{iso}} + H_{\text{an}}(3\cos^2\theta - 1)/2 \quad (3)$$

where  $H_{\text{iso}}$  is the isotropic contribution to the hyperfine magnetic field  $H_n$ , determined mainly by the Fermi contact interaction with  $s$ -electrons localized on the nucleus and polarized by the atomic spin.  $H_{\text{an}}$  is the anisotropic contribution due to the magnetic dipole-dipole interaction with localized magnetic moments of atoms and the anisotropy of the hyperfine magnetic interaction of the nucleus with the electrons of the ion core of its own atom. From Eq. (3) one can obtain a relation between the values of the hyperfine fields for the orientation of the magnetic moment of the iron atom parallel to ( $H_{\parallel}$ ) and perpendicular ( $H_{\perp}$ ) to the crystal symmetry axis with isotropic and anisotropic contributions by simple relations [24]:

$$H_{\parallel} = H_{\text{iso}} + H_{\text{an}} \text{ and } H_{\perp} = H_{\text{iso}} - H_{\text{an}}/2 \quad (4)$$

Experimental methods that can detect SSMS and observe its evolution caused, for example, by replacement of bismuth or iron by other ions or by distortions of the crystal structure are of significant importance for study perovskites based on  $\text{BiFeO}_3$  ferrite. Such methods are neutron diffraction, nuclear magnetic resonance (NMR), and nuclear gamma resonance (Mössbauer effect).

The existence of SSMS in  $\text{BiFeO}_3$  was revealed by the Mössbauer effect method on  $^{57}\text{Fe}$  nuclei [24,25]. In [25], when processing the Mössbauer spectra of  $\text{BiFeO}_3$  taking into account the lattice  $\epsilon_{\text{lat}}$  and magnetic  $\epsilon_{\text{mag}}$  contributions to the quadrupole shift, the anharmonicity parameter was estimated as  $m = 0.5$  at room temperature and  $m = 0.6$  at 90 K, i.e. SSMS is highly anharmonic. In [24], an estimate of the additional contribution from the magnetic component  $\epsilon_{\text{mag}}$  to the quadrupole shift showed that this contribution is small and can be neglected when processing the Mössbauer spectra, which leads to a decrease in the estimate of the anharmonicity parameter to  $m = 0.26$  at 4.2 K.

One of the most obvious and direct methods for observing SSMS is NMR spectroscopy. The rotation of magnetic moments modifies the line shape in such a way that the spectrum becomes frequency distributed within 2 MHz and acquires a characteristic shape with two peaks at the edges of the spectrum of different (in the general case) intensities and a gap between them. In [26], NMR spectra were obtained for samples of the  $\text{Bi}_{1-y}\text{La}_y\text{FeO}_3$  series with  $y = (0, 0.1, 0.2, 0.9 \text{ and } 1.0)$ . In the first two samples with the lowest La content, the magnetic order of the SSMS type of the cycloid type was preserved.

Up to now, only a few papers report on the effect of replacement of bismuth by rare-earth atoms on SSMS studied by neutron diffraction, NMR, or Mössbauer spectroscopy.

This work aims to systematic study of effect of replacement of trivalent bismuth atoms by trivalent lanthanum atoms on SSMS, local magnetic and electrical states of Fe atoms in the rhombohedral phase  $R3c$  of the  $\text{Bi}_{1-y}\text{La}_y\text{FeO}_3$  system ( $y = 0, 0.015, 0.03, 0.05 \text{ and } 0.10$ ) by means of NMR at 4.2 K and the Mössbauer effect at room temperature on  $^{57}\text{Fe}$  nuclei. In the present paper, we combined NMR spectroscopy at low temperature and Mössbauer spectroscopy to study the region of drastic changes in the magnetic structure of the  $\text{Bi}_{1-y}\text{La}_y\text{FeO}_3$ : the destruction of SSMS and anisotropy type change at room temperature.

## 2. Materials and methods

Polycrystalline samples of  $\text{Bi}_{1-y}\text{La}_y\text{FeO}_3$  multiferroics ( $y = 0, 0.015, 0.03, 0.05 \text{ and } 0.10$ ) with a relative content of the stable  $^{57}\text{Fe}$  isotope of 10% mol percent (for all samples except  $y = 0.10$ ) were prepared using solid-state ceramic technology. Sample with  $y = 0.10$  was characterized by a higher  $^{57}\text{Fe}$  isotope content of  $\approx 95\%$ . A mixture of oxide powders of ferrite components in appropriate proportions was pressed into tablets, which were annealed for 25 h at a temperature of 700 – 830° C in the air (with intermediate triple grinding and compression into tablets). At 830° C, the final annealing was performed, followed by the rapid cooling of the sample in air. The phase composition and structure of the samples were determined by X-ray diffraction. The samples contained impurities of  $\text{Fe}_2\text{O}_3$  and  $\text{Bi}_2\text{Fe}_4\text{O}_9$  at an amount of  $< 5\%$ .

Similar to the parent  $\text{BiFeO}_3$ , an essential local magnetic field of  $\sim 490 - 500$  kOe exists at the iron positions in all compounds investigated, which makes it possible to observe NMR signal in zero field (ZF NMR) on  $^{57}\text{Fe}$  nuclei (spin  $I = 1/2$ ). In this case, the profile of the NMR spectrum should repeat the profile of local field distribution at the iron positions up to a factor equal to the  $^{57}\text{Fe}$  gyromagnetic ratio ( $\gamma/2\pi \sim 0.138$  MHz/kOe).

The  $^{57}\text{Fe}$  NMR spectra were measured in a zero field at a liquid helium temperature since (i) no phase transitions were observed in similar compounds below room temperature [26]; (ii) cooling down to 4.2 K allows one to increase the sensitivity of the method significantly.

In all NMR measurements, the technique of detecting the spin-echo from successive  $\pi/2$  and  $\pi$  pulses with a stepwise change in frequency was used. The NMR signal was obtained by integrating the spin-echo envelope in the time domain and summing over the number of scans.

In order to suppress the contribution from  $^{209}\text{Bi}$  [27], a fairly large distance (1000  $\mu\text{s}$ ) between the  $\pi/2$  and  $\pi$  radiofrequency pulses was used in the NMR experiment. As our experiments showed, with this configuration the spin-echo from  $^{209}\text{Bi}$  almost vanishes due to fast spin-spin nuclear relaxation, while the relatively slow relaxing  $^{57}\text{Fe}$  spin-echo remains quite intense.

Relatively long  $\pi/2$  and  $\pi$  radiofrequency pulses of 10  $\mu\text{s}$  and 20  $\mu\text{s}$  were used to minimize the excitation band for each NMR measurement and to obtain a higher resolution spectrum in the frequency domain. The pulse power was optimized by maximizing an echo signal at the right peak of the major spectrum at the frequency of 75.55 MHz, the optimal power at other points of the spectrum coincided within the error limits.

Mössbauer studies were carried out at room temperature using a spectrometer operating in the constant acceleration mode with a triangular shape of the source velocity relative to the absorber at room temperature for all samples. A  $^{57}\text{Co}$  source in the Rh matrix was used. The Mössbauer spectrometer was calibrated at room temperature using a standard  $\alpha\text{-Fe}$  absorber. For processing and analysis of Mössbauer spectra, we used a cycloid type SSMS model implemented in the SpectrRelax program (described in detail in [24,28,29] as applied to process Mössbauer spectra in  $\text{BiFeO}_3$  and some ferrites based on it). The search for the optimal values of the model parameters was carried out in accordance with the maximum likelihood criterion ( $\chi^2$  criterion) by the Levenberg – Marquardt method (for more details, see [24]).

## 3. Results and discussion

### 3.1. Crystal structure

As mentioned above, the samples contained impurity phases  $\text{Fe}_2\text{O}_3$  and  $\text{Bi}_2\text{Fe}_4\text{O}_9$  at the amount of a few percents ( $< 5\%$ ). The presence of these phases in the studied samples was also confirmed by Mössbauer spectroscopy. X-ray diffraction measurements of the studied samples showed that the replacement of bismuth atoms by lanthanum atoms leads to a slight decrease in the parameters of the rhombohedral (sp.gr.

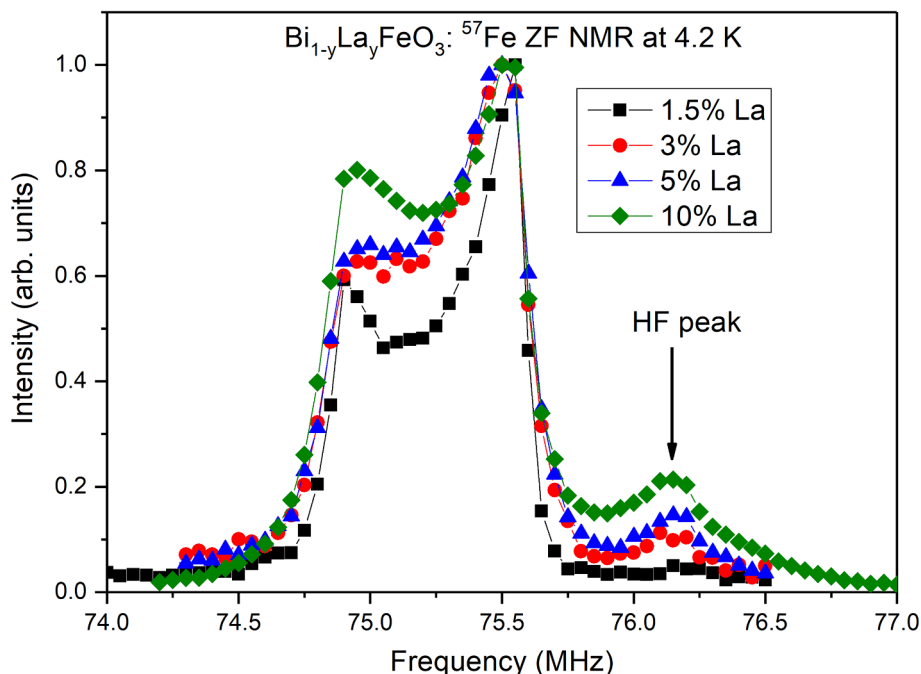


Fig. 1.  $^{57}\text{Fe}$  ZF NMR spectra of the  $\text{Bi}_{1-y}\text{La}_y\text{FeO}_3$  samples at 4.2 K. The arrow indicates the position of the high-frequency peak (see text).

$R3c$ ) lattice:  $a = b$  decreases from 5.581 Å (for  $y = 0$ ) to 5.578 Å (for  $y = 0.1$ );  $c$  decreases from 13.876 Å (for  $y = 0$ ) to 13.807 Å (for  $y = 0.1$ ). All the compounds investigated are the bulk powder samples. They do not undergo structural transition which occurs at higher content of lanthanum.

This effect is due to the difference in the effective ionic radii  $R$  for the trivalent ions of lanthanum  $\text{La}^{3+}$  and bismuth  $\text{Bi}^{3+}$  for the  $N = 12$ -oxygen coordination:  $R(\text{La}^{3+}) = 1.36$  Å and  $R(\text{Bi}^{3+}) \geq 1.4$  Å [30]. The effective radius  $R(\text{Bi}^{3+})$  was determined by linear extrapolation of the  $\text{Bi}^{3+}$  ionic radii data with 5-, 6-, and 8-coordinated oxygen environments  $N$  towards  $N = 12$ . A decrease of the studied ferrites lattice parameter  $c$  leads to compression of the lattice. This effect causes a change in the lengths and angles of the Fe–O–Fe bonds, distortion and rotation of the  $\text{FeO}_6$  octahedra [31,32].

### 3.2. Zero-field NMR

Fig. 1 shows the zero-field NMR spectra of the compositions  $\text{Bi}_{1-y}\text{La}_y\text{FeO}_3$  ( $y = 0, 0.015, 0.03, 0.05$  and  $0.10$ ) measured at 4.2 K. For all these compounds, the spectra exhibit a characteristic two-peaks structure observed in the NMR spectra of  $^{57}\text{Fe}$  nuclei in BFO [22] caused by the presence of cycloid type SSMS.

Measurements of the spin–spin relaxation rate at low-frequency and high-frequency maxima made it possible to estimate the ratio of echo intensity decay  $^{57}\text{Fe}$   $I(1000 \mu\text{s})/I(0)$  at both spectral peak positions for the used delay between pulses (Table 1). As can be seen, these relations

are close to unity within the error range, which indicates the negligibility of the relaxation inhomogeneity influence on the shape of the spectrum. The relatively large decrease for the compound with 10% substitution is associated with a significantly higher content of the  $^{57}\text{Fe}$  isotope.

An evolution of the  $^{57}\text{Fe}$  nuclei NMR spectra with an increase of La content in BFO samples is shown in Fig. 1. In particular, the intensity of the left peak increases due to iron atoms, the magnetic moments of which are perpendicular to the light axis [22]. This effect indicates a decrease in the cycloid anharmonicity parameter. This result is consistent with previously published data [26] and indicates a decrease in the effective magnetic anisotropy constant. There is also an increase in the width of the local line shape due to an increase in the heterogeneity degree of the local iron environment. It should be noted that in this case, the position and frequency range of the main spectrum almost do not change with increasing lanthanum substitution indicating that the hyperfine fields of iron nuclei  $H_{\parallel}$  and  $H_{\perp}$  remain almost unchanged.

Also, with an increase in lanthanum content, the intensity of the non-cycloid high-frequency peak increases (the HF peak in Fig. 1), the nature of which remains unclear. It corresponds to the position of iron with a local magnetic field of 554 kOe on iron nuclei. The hyperfine magnetic fields (HFMF) on  $^{57}\text{Fe}$  nuclei at 4.2 K in the most common oxides — hematite, magnetite, and maghemite — are lower, which unambiguously excludes them as potential impurities not detected by X-ray [33].

The  $^{57}\text{Fe}$  NMR spectra in the zero external magnetic field were

Table 1

A decrease in  $^{57}\text{Fe}$  spin-echo intensity due to spin–spin relaxation  $I(1000 \mu\text{s})/I(0)$  at spectral peak positions and their ratio.

	The degree of substitution of Bi for La			
	1.5%	3%	5%	10%
The 74.95 MHz peak decay $I(1000 \mu\text{s})/I(0)$	0.923(7)	0.93(2)	0.91(2)	0.58(3)
The 75.55 MHz peak decay $I(1000 \mu\text{s})/I(0)$	0.932(7)	0.932(10)	0.932(8)	0.577(17)
Ratio	0.990(11)	1.00(3)	0.98(3)	1.01(6)

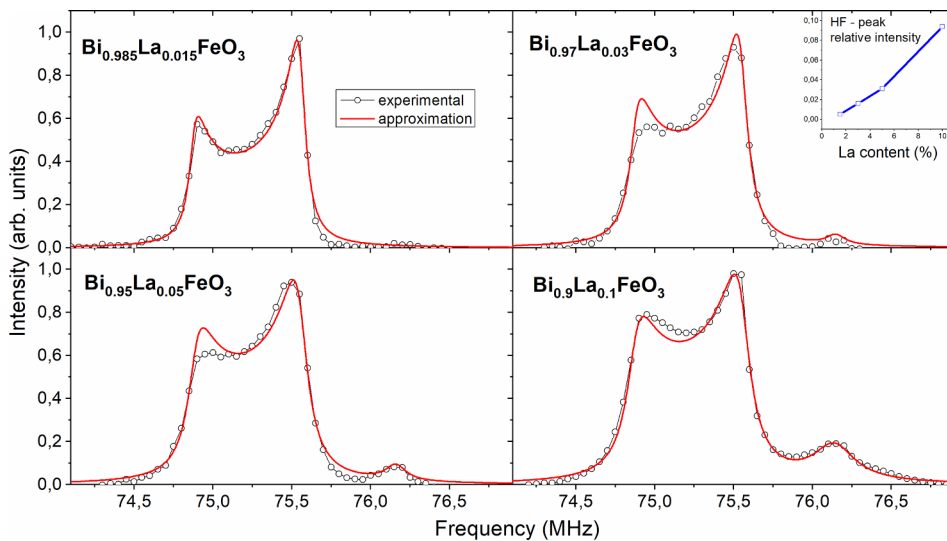


**Fig. 2.** ZF NMR spectra of  $^{57}\text{Fe}$  nuclei at 4.2 K (experimental points). The red is the approximation of the  $^{57}\text{Fe}$  NMR spectra in the framework of the anharmonic cycloid model (using Eqs. (1), (3)) in  $\text{Bi}_{1-y}\text{La}_y\text{FeO}_3$  samples. The Inset shows the relative intensity of the high-frequency peak. The sum of squared deviations was minimized using the built-in function of the PTC Mathcad software. (For interpretation of the references to colour in this figure legend, the reader is referred to the web version of this article.)

approximated by the anharmonic cycloid model (using Eqs. (1), (3)) with magnetic “easy axis” type anisotropy as in [24,28,34]. The high-frequency peak was approximated by a separate line. The approximation results (red solid curves in Fig. 2) are in a good agreement with the experiment. The obtained approximation parameters make it possible to quantitatively evaluate the changes in SSMS in the  $\text{Bi}_{1-y}\text{La}_y\text{FeO}_3$  system ( $y = 0, 0.015, 0.03, 0.05$  and  $0.10$ ).

The dependence of the anharmonicity parameter on the degree of lanthanum content is shown on the summary graph in Fig. 4 ( $m$  by ZF NMR at 4.2 K). A monotonic decrease in  $m$  with an increase in the concentration of lanthanum is observed.

The concentration dependence of the relative integral intensity of the high-frequency peak is shown in the Inset in Fig. 2. It exhibits an almost linear growth, indicating its direct connection with lanthanum concentration. Presumably, this HF-peak originates from iron atoms, in the immediate vicinity of which at least some of the eight bismuths is replaced by lanthanum. Possibly, due to the smaller ionic radius of  $\text{La}^{3+}$  compared with  $\text{Bi}^{3+}$ , the distance between such iron atoms becomes smaller than in stoichiometric  $\text{BiFeO}_3$ , which leads to an increase in HFMF on iron. Also, it might be possible that the HF peak is a part of

more complicated sub-spectrum which is hindered beneath the main spectrum.

### 3.3. Mössbauer spectroscopy

In Fig. 3, as examples, we present the Mössbauer spectra of  $^{57}\text{Fe}$  nuclei in the  $\text{Bi}_{0.985}\text{La}_{0.015}\text{FeO}_3$  (1) and  $\text{Bi}_{0.95}\text{La}_{0.05}\text{FeO}_3$  (2) multiferroics obtained at 295 K (open circles) and the results of their processing in the framework of the SSMS cycloid model in the SpectrRelax program (solid lines). The Mössbauer spectra in  $\text{Bi}_{1-y}\text{La}_y\text{FeO}_3$  multiferroics are characterized by broad asymmetric lines with specific line intensities observed in  $\text{BiFeO}_3$  multiferroic and ferrites based on it in the composition region with the  $R3c$  rhombohedral structure (for example [24,28,29]). The spectra of impurity phases are also shown in Fig. 3. The Mössbauer spectrum of the  $\text{Bi}_{0.985}\text{La}_{0.015}\text{FeO}_3$  sample contains impurity sextets from the  $\text{Fe}_2\text{O}_3$  phase at an amount of  $0.6 \pm 0.4\%$  and two doublets of the  $\text{Bi}_2\text{Fe}_4\text{O}_9$  phase with the intensity of  $1.18 \pm 0.05\%$ . The spectrum of the  $\text{Bi}_{0.95}\text{La}_{0.05}\text{FeO}_3$  sample contains  $\text{Fe}_2\text{O}_3$  impurities at an amount of  $1.2 \pm 0.7\%$  and two doublets of the  $\text{Bi}_2\text{Fe}_4\text{O}_9$  phase at an amount of  $3.8 \pm 0.06\%$ .

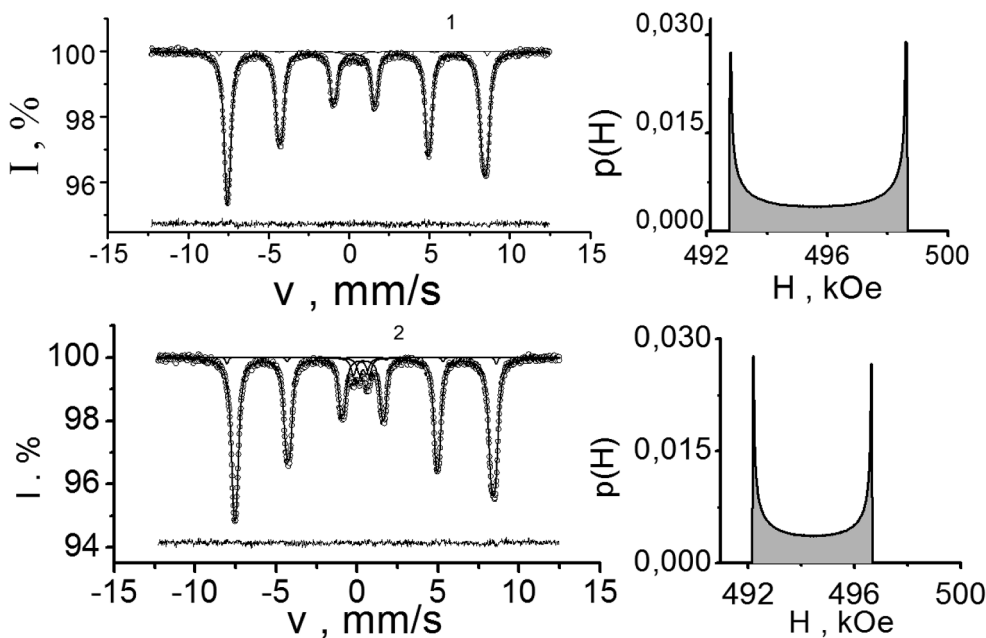


**Fig. 3.** The Mössbauer spectra of  $^{57}\text{Fe}$  nuclei (open circles) measured at room temperature and the results of their processing in the  $\text{Bi}_{0.985}\text{La}_{0.015}\text{FeO}_3$  (1) and  $\text{Bi}_{0.95}\text{La}_{0.05}\text{FeO}_3$  multiferroics (2), in the framework of the cycloid type spatial spin modulated structure (SSMS) model (SpectrRelax program). The lines passing through the experimental points are model spectra obtained by spectra analysis according to the program. The broken lines under the spectra are the difference between the experimental and model spectra. Distributions of hyperfine magnetic fields (solid lines with shaded regions)  $p(H)$  corresponding to model spectra are calculated in the framework of the cycloid type SSMS model.



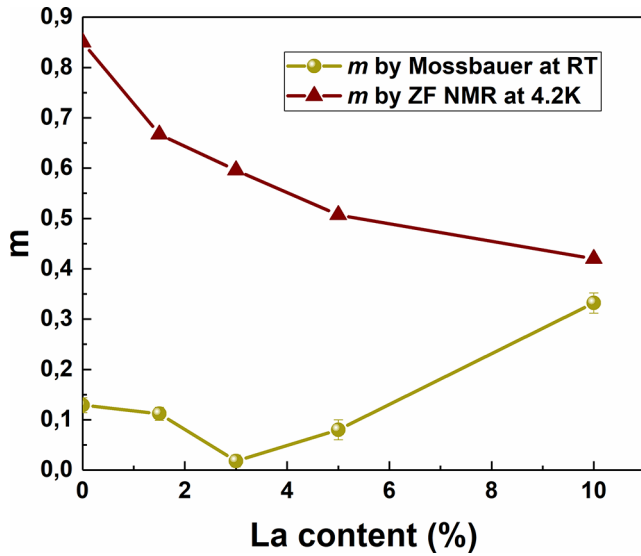


Fig. 4. Dependences of the cycloid anharmonicity parameter  $m$  on the degree of lanthanum concentration in  $\text{Bi}_{1-y}\text{La}_y\text{FeO}_3$  compounds at 4.2 K according to  $^{57}\text{Fe}$  NMR in zero field and at 300 K according to Mössbauer spectroscopy.

The Mössbauer spectra were processed in the framework of the cycloid type SSMS model using equations (1 or 2) for the angle  $\theta(x)$  between the antiferromagnetism vector and the axis of symmetry in the structure of bismuth ferrites  $\text{Bi}_{1-y}\text{La}_y\text{FeO}_3$  ( $y = 0, 0.015, 0.03, 0.05, 0.10$ ) in dependence on the  $x$  coordinate along the direction of spin modulation and the sign of the uniaxial magnetic anisotropy coefficient [35]. In [24,28,29] it was found that for  $\text{BiFeO}_3$  in the temperature range 5–300 K the angle  $\theta(x)$  is described by expression (1), depending on the sign of the effective constant of the crystalline magnetic anisotropy  $K_u$ . The authors of [25] estimated the anharmonicity parameter of SSMS in  $\text{BiFeO}_3$  when processing the Mössbauer spectra taking into account two contributions to the quadrupole shift: lattice  $\epsilon_{\text{lat}}$  and magnetic  $\epsilon_{\text{mag}}$ . At 293 K, the lattice contribution is  $\epsilon_{\text{lat}} = -0.228$  mm/s and the magnetic contribution is  $\epsilon_{\text{mag}} = 0.126$  mm/s, and the anharmonicity parameter was estimated to be  $m = 0.5$ . We measured the lattice contributions of  $\epsilon_{\text{lat}}$  to quadrupole splitting from Mössbauer spectra at temperatures above the Neel temperature  $T_N$ , in  $\text{BiFeO}_3$  ferrites (at  $T = 670$  K) and  $\text{Bi}_{0.95}\text{La}_{0.05}\text{FeO}_3$  (at  $T = 663$  K):  $\epsilon_{\text{lat}} = 0.2172 (\pm 0.0007)$  mm/s (for  $\text{BiFeO}_3$ ) and  $\epsilon_{\text{lat}} = 0.2133 (\pm 0.0008)$  mm/s (for  $\text{Bi}_{0.95}\text{La}_{0.05}\text{FeO}_3$ ). The value  $\epsilon_{\text{lat}} = 0.254$  (2) mm/s at 4.2 K obtained in [24] is close to the lattice contribution  $\epsilon_{\text{lat}}$  measured in  $\text{BiFeO}_3$  at a temperature of 650 K.

The Mössbauer spectra in the  $\text{Bi}_{1-y}\text{La}_y\text{FeO}_3$  multiferroic system ( $y = 0, 0.015, 0.03, 0.05$ , and  $0.10$ ) were analyzed using the equation (1 or 2) taking into account the fact that the magnetic contribution to the quadrupole splitting is equal to zero  $\epsilon_{\text{mag}} \equiv 0$ . As a result of the Mössbauer spectra analysis in the framework of the cycloid type SSMS model, we obtained data on the anharmonicity parameters  $m$  and the HFMF distributions  $p(H_n)$  at room temperature depending on the content of lanthanum atoms. The best agreement of the experimental and model spectra for compositions  $y = 0 - 0.03$  was obtained by processing the spectrum according to equation (1), while for compositions  $y = 0.05$  and  $0.10$  – when processing the spectra according to equation (2). Fig. 3.1 shows that in the distribution  $p(H_n)$  for the composition  $y = 0.015$ , the intensity of the left peak (74.95 MHz)  $I_L$  is less than the intensity of the right peak  $I_R$  (75.55 MHz). In Fig. 3.2 one can see that the  $I_R$  intensity is less than  $I_L$ . This means that the magnetic state of multiferroics with composition  $y = 0 - 0.03$  is described by a cycloid type SSMS with a positive uniaxial effective magnetic constant  $K_u > 0$  (“easy axis”), and the magnetic state of multiferroics with compositions  $y = 0.05$  and  $0.10$  cycloid type SSMS is described with a negative

effective magnetic constant  $K_u < 0$  (“easy plane”). The anharmonicity parameter  $m$  at room temperature in the composition range  $y = 0.03 - 0.05$  is close to zero. SSMS in this area of compositions is harmonic.

Fig. 4 shows the concentration dependences of the anharmonicity parameter in  $\text{Bi}_{1-y}\text{La}_y\text{FeO}_3$  multiferroics ( $y = 0, 0.015, 0.03, 0.05$ , and  $0.10$ ) determined at 4.2 K by the NMR method, and at room temperature measured by the Mössbauer spectroscopy on  $^{57}\text{Fe}$  nuclei. As can be seen from the figure when bismuth atoms are replaced by lanthanum atoms, the anharmonicity parameter  $m$  measured by NMR decreases from 0.85 at  $y = 0$  to 0.42 at  $y = 0.10$ . The shape of the NMR spectra shows that in this temperature range in  $\text{Bi}_{1-y}\text{La}_y\text{FeO}_3$  multiferroics ( $y = 0.03, 0.05$ , and  $0.10$ ) a cycloid type SSMS exists. This SSMS is characterized by a positive effective uniaxial magnetic anisotropy constant  $K_u > 0$ . The parameters  $m$  obtained by processing the NMR spectra (measured at 4.2 K) according to equation (1) are shown in Fig. 4.

The anharmonicity parameter  $m$  retrieved from the Mössbauer spectroscopy at room temperature for compositions  $y = 0.00 - 0.03$  decreases with increasing lanthanum content. For compositions  $y = 0.03 - 0.05$ , the parameter  $m \approx 0$  and, therefore, the constant  $K_u \approx 0$ . Then  $m$  increases to 0.32 at  $y = 0.10$ . For ferrites  $\text{Bi}_{0.95}\text{La}_{0.05}\text{FeO}_3$  and  $\text{Bi}_{0.90}\text{La}_{0.10}\text{FeO}_3$ , the best agreement (the smallest parameter  $\chi^2$ ) was obtained by processing the spectra according to equation (2). This means that for the ferrites  $\text{Bi}_{0.95}\text{La}_{0.05}\text{FeO}_3$  and  $\text{Bi}_{0.90}\text{La}_{0.10}\text{FeO}_3$  the effective magnetic anisotropy constant is negative  $K_u < 0$ . As follows from Fig. 4, the change of sign of the anisotropy constant from positive to negative at room temperature occurs at a La concentration  $y \approx 0.03$  where the parameter  $m = 0$  and SSMS becomes harmonic.

In paper [28] the authors used Mössbauer spectroscopy to study the temperature dependence of  $m$  in multiferroic  $\text{BiFeO}_3$ . With temperature increase from 4.8 K, the parameter  $m$  decreases from  $m = 0.26$  to  $m = 0$  at  $T_{\text{inv}} \approx 330$  K. With temperature increase above  $T_{\text{inv}}$ ,  $m$  increases to  $m \approx 0.6$  at  $T = 585$  K. In this paper the authors demonstrate that when  $T < T_{\text{inv}}$  the SSMS in  $\text{BiFeO}_3$  is characterized by  $K_u > 0$  while when  $T > T_{\text{inv}}$   $K_u < 0$ . At temperature  $T_{\text{inv}} \approx 330$  K, the parameter  $m = 0$ . The effect of sign switching of the effective  $K_u$  magnetic anisotropy constant is explained by different temperature dependences of competing contributions to the effective magnetic anisotropy constant. One contribution is produced by the antiferromagnetic system without taking into account the canting of the magnetic sublattices, and the other contribution is produced by weak ferromagnetism due to the Dzyaloshinsky-Moria interaction (which determines the canting of the magnetic sublattices) [28].

The anharmonicity parameter  $m$  is related to the spatial spin-modulated wavelength  $\lambda$ , the exchange stiffness  $A$ , and the effective magnetic anisotropy constant  $K_u$  [22,26]:  $m \sim (\lambda^2 K_u/A)$ . Unfortunately, there is no data in the literature of the cycloid length  $\lambda$  dependence on the composition in the  $\text{Bi}_{1-y}\text{La}_y\text{FeO}_3$  ferrite system ( $y = 0 - 0.10$ ). For comparison, when replacing trivalent iron atoms by trivalent manganese atoms, the parameter  $\lambda$  increased slightly, from 620 Å to 680 Å at Mn concentration of 10% [36]. The exchange stiffness parameter  $A$  is determined by the Néel temperature  $T_N$  ( $A \sim T_N$ ). For  $\text{BiFeO}_3$  the temperature  $T_N = 640$  K and for  $\text{Bi}_{0.9}\text{La}_{0.1}\text{FeO}_3$  it is 655 K. In this regard, we can assume that the effect of a change in the cycloid period  $\lambda$  and exchange stiffness  $A$  on a decrease in the anharmonicity parameter  $m$  in  $\text{Bi}_{1-y}\text{La}_y\text{FeO}_3$  ferrites ( $y = 0 - 0.10$ ) is insignificant, and the main contribution to the change in the parameter  $m$  with increasing lanthanum content is made by the dependence on the composition of the effective magnetic anisotropy constant  $K_u$ . Thus, a decrease in the anharmonicity parameter  $m$  caused by the replacement of trivalent bismuth atoms by trivalent lanthanum atoms in  $\text{Bi}_{1-y}\text{La}_y\text{FeO}_3$  multiferroics ( $y = 0, 0.015, 0.03$ ) and an increase in  $m$  parameter in  $\text{Bi}_{1-y}\text{La}_y\text{FeO}_3$  multiferroics ( $y = 0.05$  and  $0.10$ ) are mainly due to concentration changes of both the magnitude and the sign of the effective magnetic anisotropy constant  $K_u$ .

#### 4. Conclusions

X-ray diffraction studies of  $\text{Bi}_{1-y}\text{La}_y\text{FeO}_3$  multiferroic samples ( $y = 0, 0.015, 0.03, 0.05$  and  $0.10$ ) defined the crystal structure of the samples as rhombohedral with the space group  $R3c$ . The lattice parameters decrease with increasing lanthanum content. This effect is caused by a smaller value of the effective ionic radius  $R$  of trivalent  $\text{La}^{3+}$  lanthanum ions relative to the radius  $R$  of bismuth  $\text{Bi}^{3+}$  for  $N = 12$ -oxygen environment.

The magnetic structure of  $\text{Bi}_{1-y}\text{La}_y\text{FeO}_3$  multiferroics ( $y = 0, 0.015, 0.03, 0.05$ , and  $0.10$ ) was studied by nuclear magnetic resonance at  $4.2$  K and the Mossbauer effect at room temperature on  $^{57}\text{Fe}$  nuclei. It has been found that in the observed composition range, there is a cycloid type SSMS. A study of the concentration dependence of the anharmonicity parameter  $m$  showed that at the liquid helium temperature the magnetic state of multiferroics in the composition region  $y = 0 - 0.10$  is described by a cycloid type SSMS with a positive effective uniaxial constant of magnetic anisotropy  $K_u > 0$  ("easy axis"). At  $4.2$  K with an increase in the La concentration the anharmonicity parameter decreases monotonically.

NMR experiments revealed that when La replaces Bi in the  $\text{BiFeO}_3$  multiferroic, Fe atoms located directly near the substituting La atoms induce a higher local magnetic field which leads to the appearance of an additional high-frequency peak on the  $^{57}\text{Fe}$  NMR spectra.

At room temperature the magnetic state of multiferroics of compositions  $y = 0 - 0.03$  is also described by SSMS with a positive effective uniaxial magnetic constant  $K_u > 0$  ("easy axis") as evidenced by Mossbauer spectroscopy study. However, in the composition range  $y = 0.05 - 0.10$  the SSMS exhibits a negative effective magnetic anisotropy constant  $K_u < 0$  ("easy plane"). The anharmonicity parameter  $m$  at room temperature in the composition range  $y = 0.03 - 0.05$  is close to zero. SSMS in this area of compositions is more harmonic. The concentration and temperature changes of the anharmonicity parameter  $m$  upon replacement of trivalent bismuth atoms by trivalent lanthanum atoms in  $\text{Bi}_{1-y}\text{La}_y\text{FeO}_3$  multiferroics ( $y = 0 - 0.10$ ) are mainly associated with concentration and temperature changes in both the magnitude and the sign of the effective magnetic anisotropy constant  $K_u$ . Changes of the  $K_u$  constant are caused by different temperature and concentration dependences of competing contributions to the effective magnetic anisotropy constant: a contribution from the antiferromagnetic system without taking into account the canting of the magnetic sublattices and weak ferromagnetism due to the Dzyaloshinsky-Moria interaction (which determines the canting angle of the magnetic sublattices).

#### CRedit authorship contribution statement

**V.S. Pokatilov:** Conceptualization, Formal analysis. **A.O. Makarova:** Data curation. **A.A. Gippius:** Project administration, Supervision. **A.V. Tkachev:** Software, Data curation. **S.V. Zhurenko:** Investigation, Software. **A.N. Bagdinova:** Visualization. **N.E. Gervits:** Writing - original draft, Writing - review & editing, Methodology.

#### Declaration of Competing Interest

The authors declare that they have no known competing financial interests or personal relationships that could have appeared to influence the work reported in this paper.

#### Acknowledgements

V.S. Pokatilov and A.O. Makarova appreciate the support of the RFBR grant No. 20-02-00795. N.E. Gervits, A.A. Gippius, A.V. Tkachev and S.V. Zhurenko are grateful for the support of the RFBR grant No. 17-52-80036; A.A. Gippius and A.N. Bagdinova thank the Russian

Foundation for Basic Research (RFBR) for the financial support of the project № 19-29-10007. Also, the team of authors is grateful for the fruitful discussion with S.N. Polulyakh.

#### References

- [1] A.M. Kadomtseva, Y.F. Popov, A.P. Pyatakov, G.P. Vorob'ev, A.K. Zvezdin, D. Viehland, Phase transitions in multiferroic  $\text{BiFeO}_3$  crystals, thin-layers, and ceramics: Enduring potential for a single phase, room-temperature magnetoelectric "holy grail, *Phase Trans.* 79 (2006) 1019–1042, <https://doi.org/10.1080/01411590601067235>.
- [2] S.V. V. Khikhlovskiy, G. Blake, The renaissance of multiferroics: bismuth ferrite ( $\text{BiFeO}_3$ )-a candidate multiferroic material in nanoscience, 2010.
- [3] G. Catalan, J.F. Scott, Physics and applications of bismuth ferrite, *Adv. Mater.* 21 (2009) 2463–2485, <https://doi.org/10.1002/adma.200802849>.
- [4] M. Bibes, A. Barthélémy, Multiferroics: Towards a magnetoelectric memory, *Nat. Mater.* 7 (2008) 425–426, <https://doi.org/10.1038/nmat2189>.
- [5] F. Kubel, H. Schmid, Structure of a ferroelectric and ferroelastic monodomain crystal of the perovskite  $\text{BiFeO}_3$ , *Acta Crystallogr. Sect. B.* 46 (1990) 698–702, <https://doi.org/10.1107/S0108768190006887>.
- [6] C. Michel, J.M. Moreau, G.D. Achenbach, R. Gerson, W.J. James, The atomic structure of  $\text{BiFeO}_3$ , *Solid State Commun.* 7 (1969) 701–704, [https://doi.org/10.1016/0038-1098\(69\)90597-3](https://doi.org/10.1016/0038-1098(69)90597-3).
- [7] I. Sosnowska, T.P. Neumaier, E. Steichele, Spiral magnetic ordering in bismuth ferrite, *J. Phys. C: Solid State Phys.* 15 (1982) 4835–4846, <https://doi.org/10.1088/0022-3719/15/23/020>.
- [8] Y. Popov, A. Zvezdin, G. Vorobev, A. Kadomtseva, V. Murashev, D. Rakov, Linear magnetoelectric effect and phase-transitions in bismuth ferrite,  $\text{BiFeO}_3$ , *JETP Lett.* 57 (1993) 69–73 (accessed December 11, 2019), [http://www.jetpletters.ac.ru/ps/1174/article\\_17734.pdf](http://www.jetpletters.ac.ru/ps/1174/article_17734.pdf).
- [9] A.M. Kadomtseva, Y.F. Popov, G.P. Vorob'ev, A.K. Zvezdin, Spin density wave and field induced phase transitions in magnetoelectric antiferromagnets, *Phys. B Phys. Condens. Matter.* 211 (1995) 327–330, [https://doi.org/10.1016/0921-4526\(94\)01051-2](https://doi.org/10.1016/0921-4526(94)01051-2).
- [10] C. Tab Ares-Muñoz, J.P. Rivera, A. Bezings, A. Monnier, H. Schmid, Measurement of the quadratic magnetoelectric effect on single crystalline  $\text{BiFeO}_3$ , *Jpn. J. Appl. Phys.* 24 (1985) 1051–1053, <https://doi.org/10.7567/JJAPS.24S2.1051>.
- [11] F. Huang, Z. Wang, X. Lu, J. Zhang, K. Min, W. Lin, R. Ti, T. Xu, J. He, C. Yue, J. Zhu, Peculiar magnetism of  $\text{BiFeO}_3$  nanoparticles with size approaching the period of the spiral spin structure, *Sci. Rep.* 3 (2013) 1–7, <https://doi.org/10.1038/srep02907>.
- [12] F. Zavaliche, S.Y. Yang, T. Zhao, Y.H. Chu, M.P. Cruz, C.B. Eom, R. Ramesh, Multiferroic  $\text{BiFeO}_3$  films: Domain structure and polarization dynamics, *Phase Trans.* 79 (2006) 991–1017, <https://doi.org/10.1080/01411590601067144>.
- [13] C.Y. Kuo, Z. Hu, J.C. Yang, S.C. Liao, Y.L. Huang, R.K. Vasudevan, M.B. Okatan, S. Jesse, S.V. Kalinin, L. Li, H.J. Liu, C.H. Lai, T.W. Pi, S. Agrestini, K. Chen, P. Ohresser, A. Tanaka, L.H. Tjeng, Y.H. Chu, Single-domain multiferroic  $\text{BiFeO}_3$  films, *Nat. Commun.* 7 (2016), <https://doi.org/10.1038/ncomms12712>.
- [14] S. Bordács, D.G. Farkas, J.S. White, R. Cubitt, L. Debeer-Schmitt, T. Ito, I. Kézsmárki, Magnetic field control of cycloidal domains and electric polarization in multiferroic  $\text{BiFeO}_3$ , *Phys. Rev. Lett.* 120 (2018) 147203, <https://doi.org/10.1103/PhysRevLett.120.147203>.
- [15] G. Le Bras, D. Colson, A. Forget, N. Genand-Riondet, R. Tourbot, P. Bonville, Magnetization and magnetoelectric effect in  $\text{Bi}_{1-x}\text{La}_x\text{FeO}_3$  ( $0 \leq x \leq 0.15$ ), *Phys. Rev. B - Condens. Matter Phys.* 80 (2009), <https://doi.org/10.1103/PhysRevB.80.134417>.
- [16] P.T. Lin, X. Li, L. Zhang, J.H. Yin, X.W. Cheng, Z.H. Wang, Y.C. Wu, G.H. Wu, Lapped  $\text{BiFeO}_3$ : Synthesis and multiferroic property study, *Chin. Phys. B.* 23 (2014), <https://doi.org/10.1088/1674-1056/23/4/047701>.
- [17] Z.V. Gabbasova, M.D. Kuz'min, A.K. Zvezdin, I.S. Dubenko, V.A. Murashov, D.N. Rakov, I.B. Krynetsky,  $\text{Bi}_{1-x}\text{R}_x\text{FeO}_3$  ( $R = \text{rare earth}$ ): a family of novel magnetoelectrics, *Phys. Lett. A* 158 (1991) 491–498, [https://doi.org/10.1016/0375-9601\(91\)90467-M](https://doi.org/10.1016/0375-9601(91)90467-M).
- [18] Y. Wang, R.Y. Zheng, C.H. Sim, J. Wang, Charged defects and their effects on electrical behavior in  $\text{Bi}_{1-x}\text{La}_x\text{FeO}_3$  thin films, *J. Appl. Phys.* 105 (2009), <https://doi.org/10.1063/1.3065473>.
- [19] S.M. Hossain, A. Mukherjee, S. Chakraborty, S.M. Yusuf, S. Basu, M. Pal, Enhanced Multiferroic Properties of Nanocrystalline La-Doped  $\text{BiFeO}_3$ , *Mater. Focus.* 2 (2013) 92–98, <https://doi.org/10.1166/mat.2013.1057>.
- [20] A.K. Ghosh, G.D. Dwivedi, B. Chatterjee, B. Rana, A. Barman, S. Chatterjee, H.D. Yang, Role of codoping on multiferroic properties at room temperature in  $\text{BiFeO}_3$  ceramic, *Solid State Commun.* 166 (2013) 22–26, <https://doi.org/10.1016/j.ssc.2013.04.029>.
- [21] X. Yao, C. Wang, S. Tian, Y. Zhou, X. Li, C. Ge, E. Jia Guo, M. He, X. Bai, P. Gao, G. Yang, K. Jin, Growth and physical properties of  $\text{BiFeO}_3$  thin films directly on Si substrate, *J. Cryst. Growth* 522 (2019) 110–116, <https://doi.org/10.1016/j.jcrysgro.2019.06.017>.
- [22] A.V. Zalesky, A.A. Frolov, T.A. Khimich, A.A. Bush, V.S. Pokatilov, A.K. Zvezdin,  $^{57}\text{Fe}$  NMR study of spin-modulated magnetic structure in  $\text{BiFeO}_3$ , *Europhys. Lett.* 50 (2000) 547–551, <https://doi.org/10.1209/EPL/12000-00304-5>.
- [23] I. Sosnowska, A.K. Zvezdin, Origin of the long period magnetic ordering in  $\text{BiFeO}_3$ , *J. Magn. Magn. Mater.* 140–144 (1995) 167–168, [https://doi.org/10.1016/0304-8853\(94\)01120-6](https://doi.org/10.1016/0304-8853(94)01120-6).
- [24] V.S. Rusakov, V.S. Pokatilov, A.S. Sigov, M.E. Matsnev, T.V. Gubaidulina,

- Diagnostics of a spatial spin-modulated structure using nuclear magnetic resonance and Mössbauer spectroscopy, *JETP Lett.* 100 (2014) 463–469, <https://doi.org/10.1134/S0021364014190102>.
- [25] A. Palewicz, T. Szumiata, R. Przeniosło, I. Sosnowska, I. Margiolaki, Search for new modulations in the BiFeO<sub>3</sub> structure: SR diffraction and Mössbauer studies, *Solid State Commun.* 140 (2006) 359–363, <https://doi.org/10.1016/j.ssc.2006.08.046>.
- [26] A.V. Zalesskiĭ, A.A. Frolov, T.A. Khimich, A.A. Bush, Composition-induced transition of spin-modulated structure into a uniform antiferromagnetic state in a Bi<sub>1-x</sub>La<sub>x</sub>FeO<sub>3</sub> system studied using <sup>57</sup>Fe NMR, *Phys. Solid State* 45 (2003) 141–145, <https://doi.org/10.1134/1.1537425>.
- [27] A.A. Bush, A.A. Gippius, A.V. Zalesskiĭ, E.N. Morozova, <sup>209</sup>Bi NMR spectrum of BiFeO<sub>3</sub> in the presence of spatial modulation of hyperfine fields, *JETP Lett.* 78 (2003) 389–392, <https://doi.org/10.1134/1.1630133>.
- [28] V. Rusakov, V. Pokatilov, A. Sigov, M. Matsnev, A. Pyatakov, Temperature Mössbauer study of the spatial spin-modulated structure in the multiferroic BiFeO<sub>3</sub>, *EPJ Web Conf.* 185 (2018) 07010, <https://doi.org/10.1051/EPJCONF/201818507010>.
- [29] V.S. Rusakov, V.S. Pokatilov, A.S. Sigov, M.E. Matsnev, A.M. Gapochka, T.Y. Kiseleva, A.E. Komarov, M.S. Shatokhin, A.O. Makarova, Spatial spin-modulated structure and hyperfine interactions of <sup>57</sup>Fe nuclei in multiferroics BiFe<sub>1-x</sub>T<sub>x</sub>O<sub>3</sub> (T = Sc, Mn; x = 0, 0.05), *Phys. Solid State* 58 (2016) 102–107, <https://doi.org/10.1134/S1063783416010261>.
- [30] R.D. Shannon, Revised effective ionic radii and systematic studies of interatomic distances in halides and chalcogenides, *Acta Crystallogr. Sect. A.* 32 (1976) 751–767, <https://doi.org/10.1107/S0567739476001551>.
- [31] M. Rahimkhani, D.S. Khoshnood, The Influence of La and Ho Substitution on Structural, Micro Structural and Magnetic Properties of BiFeO<sub>3</sub> Nanopowders, *Procedia Mater. Sci.* 11 (2015) 238–241, <https://doi.org/10.1016/j.mspro.2015.11.121>.
- [32] K. Sen, K. Singh, A. Gautam, M. Singh, Dispersion studies of La substitution on dielectric and ferroelectric properties of multiferroic BiFeO<sub>3</sub> ceramic, *Ceram. Int.* 38 (2012) 243–249, <https://doi.org/10.1016/j.ceramint.2011.06.059>.
- [33] N.E. Gervits, A.A. Gippius, A.V. Tkachev, E.I. Demikhov, S.S. Starchikov, I.S. Lyubutin, A.L. Vasiliev, V.P. Chekhonin, M.A. Abakumov, A.S. Semkina, A.G. Mazhuga, Magnetic properties of biofunctionalized iron oxide nanoparticles as magnetic resonance imaging contrast agents, *Beilstein J. Nanotechnol.* 10 (2019) 1964–1972, <https://doi.org/10.3762/bjnano.10.193>.
- [34] A.A.A. Gippius, A.V.V. Tkachev, N.E.E. Gervits, V.S.S. Pokatilov, A.O.O. Konovalova, A.S.S. Sigov, Evolution of spin-modulated magnetic structure in multiferroic compound Bi<sub>(1-x)</sub>Sr<sub>x</sub>FeO<sub>3</sub>, *Solid State Commun.* 152 (2012) 552–556, <https://doi.org/10.1016/j.ssc.2011.12.028>.
- [35] M.M. Tehranchi, N.F. Kubrakov, A.K. Zvezdin, Spin-flop and incommensurate structures in magnetic ferroelectrics, *Ferroelectrics* 204 (1997) 181–188, <https://doi.org/10.1080/00150199708222198>.
- [36] I. Sosnowska, W. Schäfer, W. Kockelmann, K.H. Andersen, I.O. Troyanchuk, Crystal structure and spiral magnetic ordering of BiFeO<sub>3</sub> doped with manganese, *Appl. Phys. A Mater. Sci. Process.* 74 (2002), <https://doi.org/10.1007/s003390201604>.